

H. Cesiulis\*, N. Tsyntsaru\*\*, A. Budreika\*, N. Skridaila\*

## **ELECTRODEPOSITION OF CoMo AND CoMoP ALLOYS FROM THE WEAKLY ACIDIC SOLUTIONS**

*\*Vilnius University, Dept. Phys.Chem.,  
Naugarduko 24, Vilnius LT-03225, Lithuania, henrikas.cesiulis@chf.vu.lt*

*\*\* Institute of Applied Physics of ASM,  
Akademiei str. 5, Chisinau, MD-2028, Republic of Moldova*

### **Introduction**

The procedures for the electrodeposition of Co-Mo alloys have been intensively developed because these alloys possess premium hardness, high melting point, reasonable resistance to corrosion and wear of these coatings [1–5]. Some of them also show catalytic properties and might be used for hydrogen generation [6–12]. Introduction of 5 to 11 wt % molybdenum into cobalt electrodeposits leads to obtaining of materials with good low-coercitivity properties [13–16]. The magnetic and mechanical properties of Co-Mo alloys make them promising for application in the microelectronics, e.g. in microelectromechanical systems (MEMS) applications. The electrochemical forming of MEMS have many advantages over other physical processes, such as a room temperature operation, low energy requirements, fast deposition rates, fairly uniform deposition over complicated shapes, low cost, simple scale-up and easily maintained equipment. MEMS are integrated micro devices or systems combining electrical and mechanical components fabricated using integrated circuit (IC) compatible batch-processing techniques and range in size from micrometers to millimeters. The properties of the deposit can be “tailored” by controlling solution compositions and deposition parameters [17]. In this case the deposition processes have to be compatible with other MEMS processing operations. The magnetic deposits must have good adhesion, low stress, corrosion resistance and thermal stability at operating temperatures without contaminating ICs. In addition, the stresses in deposit is important factor, because may result cracks or deformations of electroformed MEMS devices.

Several types of baths are used for the electrodeposition of Co-Mo films. Co-Mo alloys are deposited from citrate and citrate-ammonium electrolytes [13–16]. The theoretical model proposed in [18] of deposition from citrate baths allow to describe the behavior of cobalt-molybdenum electrodeposition process. Different hypotheses presented in [18] that deduced the theoretical expressions and compare the theoretical and experimental *i-t* curves are available. Also a mathematical model of the induced co-deposition of molybdenum and the iron family metals from citrate-ammonia baths was proposed in [19, 20]. The appearance of obtained coatings from a citrate - chloride bath was worse than in the case of the coatings obtained from a citrate-sulphate bath. Probably, it was the result of chloride ions adsorption on the Co-Mo deposit during electrodeposition process [21]. The citrate and citrate ammonia bath are widely used [13, 14, 22, 23]. The amount of Mo in alloys electroplated from these baths contains about 20 at % of molybdenum. The pH of the solution has effect on the current efficiency, morphology and composition of the alloys. The alloy composition is just slightly dependent from solution pH, but at higher pH values powder-like coatings are formed [24]. The ammonia salts is used to intensify the process, but for Co alloys instead of ammonia salts the hydrazine could be used [25]. Weakly alkaline pyrophosphate baths are also used for electrodeposition of molybdenum alloys [26–28]. Comparative characteristics of the Co-Mo alloys electroplating from citrate, pyrophosphate and mixed citrate-pyrophosphate baths are given in [29]. The research of current efficiency influence on composition, morphology and microhardness of Co-Mo alloys deposited from citrate bath with Na<sub>2</sub>EDTA is available for e.g. in [30]. Also investigation on practical use of the electroplating of ternary alloys containing molybdenum and phosphorus from the same type of baths has been carried out. The relation between the composition, morphology, corrosion resistance and physicomechanical properties of CoMoP coatings has been studied in [31, 32].

The aim of the present study is to investigate the electrodeposition of Co-Mo and Co-Mo-P alloys from the weakly acidic citrate bath and clarify factors influencing the deposition rate and composition of ob-

taining alloys, as well as their structure. The values of pH are concerned taking into account the potential applicability of the bath for template-assisted electroforming of devices using photoresist layers unstable in alkaline media, e.g. AZ4562.

## Experimental

Electrodeposition was carried out from the electrolytes of the following composition:

Solution 1:  $\text{CoSO}_4$  (0.3 M) +  $\text{Na}_3\text{Citr.}$  (0.2 M) +  $\text{Na}_2\text{MoO}_4$  (0,005 M);

Solution 2:  $\text{CoSO}_4$  (0.3 M) +  $\text{Na}_3\text{Citr.}$  (0.2 M) +  $\text{Na}_2\text{MoO}_4$  (0,012 M);

Solution 3:  $\text{CoSO}_4$  (0.3 M) +  $\text{Na}_3\text{Citr.}$  (0.2 M) +  $\text{Na}_2\text{MoO}_4$  (0,012 M) +  $\text{NaH}_2\text{PO}_2$  (0,1M);

Solution 4:  $\text{CoSO}_4$  (0.3 M) +  $\text{Na}_3\text{Citr.}$  (0.2 M).

All experiments were carried out at the temperature of 20 °C and in the range of current densities of 2.5 – 25  $\text{mA/cm}^2$  pH 3-5. For the deposition a plating cell with two separated anodic compartments was used. The substrate was made of pure copper foil of working area 2–8  $\text{cm}^2$ . Before the electrodeposition the surface was mechanically polished, degreased and then activated in dilute sulfuric acid. A platinum plated titanium mesh was used as the counter electrode. The total current density was controlled using AUTOLAB302 system.

The coating morphology was investigated by scanning electron microscopy (Philips XL 30 FEG). Qualitative elemental analysis of the obtained alloys was carried out by energy-dispersive X-ray spectroscopy (EDS). X-ray diffraction analyses were performed to characterize the electrodeposited coatings. A Dron (type 3.0) instrument with Ni filtered Cu-K $\alpha$ 1 radiation operated at 30 kV and 30 mA ( $\lambda=1.54056 \text{ \AA}$ ) was used at a continuous scan speed of 0.02° 2 $\theta$  s<sup>-1</sup>. The obtained XRD patterns were filtered from Cu signals.

## Results and discussions

### 1.1. Co-Mo alloys study

**1.1.1. Current Efficiency and Deposition Rate.** Figures 1 and 2 show the dependences of current efficiency and the deposition rate on the current density of Co-Mo alloys obtained from Solution 1 and 2. For comparison, the Fig. 3 and 4 show the dependence of the current efficiency and the deposition rate of pure Co coatings from electrolyte:  $\text{CoSO}_4$  (0.3 M) +  $\text{Na}_3\text{Citr}$  (0.2 M) at the same current densities. One can be seen that the deposition rates for cobalt–molybdenum coatings are sufficiently lower; this is chiefly due to lower hydrogen overvoltage on Mo-containing electrodes. It is also obvious that the investigating solution have a high throwing power, because in a wide range of applied current densities the current efficiency falling down with the increase in current density at pH 4 and 5 (Fig. 1). At pH 5 (Fig. 2) this dependence give the practically identical rate of deposition that is favourable for electrodeposition in recesses where local current density can be different at this is usually effect the uniformity of deposit grow. From this point of view the deposition of pure Co should give worse results (Fig. 4), nevertheless that deposition rate is higher for this process.

The change of electrodeposition potential by ~0.1-0.15V is evident at the higher current densities and at the beginning of electrodeposition (see Fig. 5). The rise of electrodeposition potential is caused probably by the enrichment of Mo in the depositing alloy after Cu substrate had been covered by first layers of Co-Mo. Further, the electrodeposition potential becomes stable enough, and compositionally uniform alloys can be obtained through entire film thickness of Co-Mo.

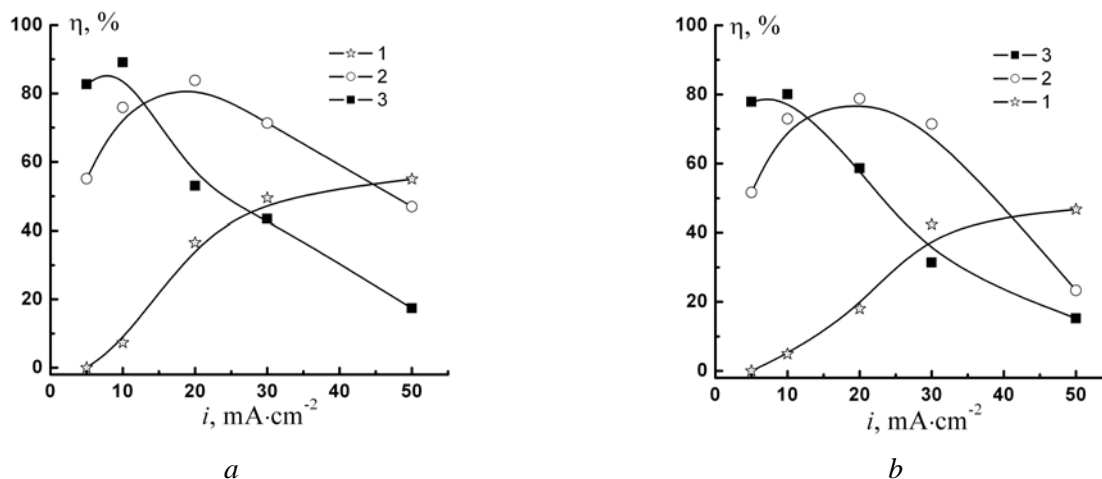


Fig. 1. Influence of current density on current efficiency at various pH for Solution 1 (a) and Solution 2 (b), 1 – pH 3, 2 – pH 4, 3 – pH 5

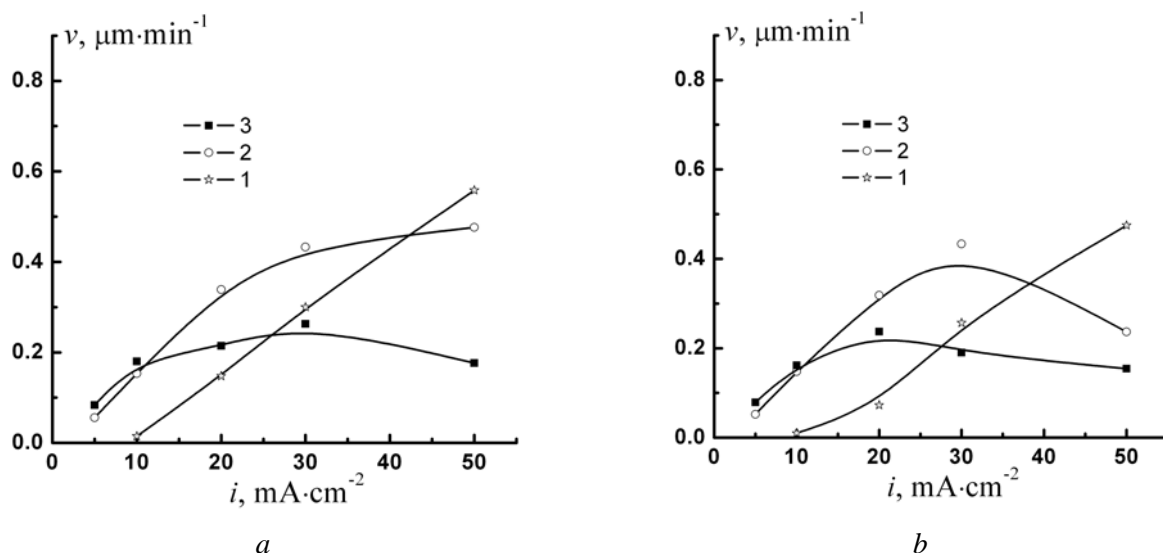


Fig. 2. Influence of current density on deposition rate at various pH for Solution 1 (a) and Solution 2 (b), 1 – pH 3, 2 – pH 4, 3 – pH 5

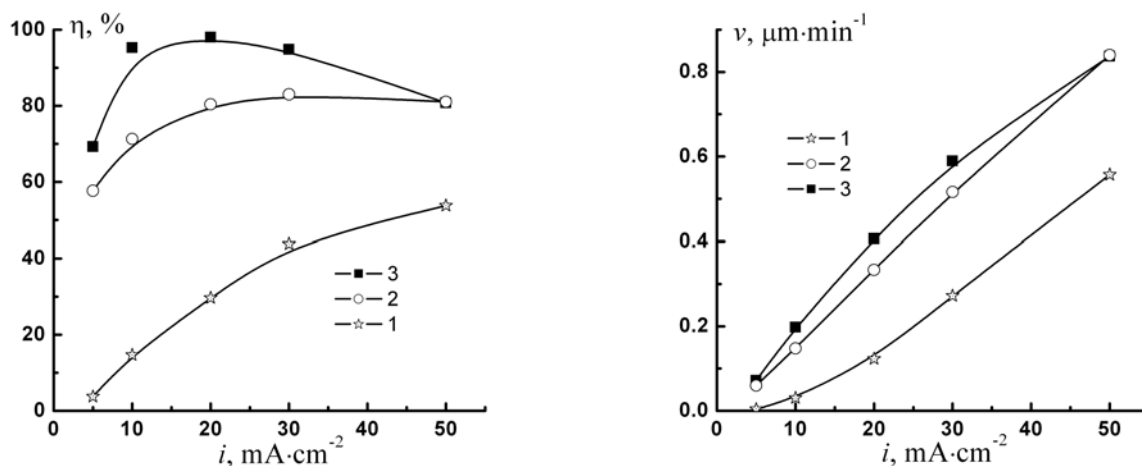


Fig. 3. Influence of current density on current efficiency at various pH for pure Co electrodeposition from Solution 4, 1 – pH 3, 2 – pH 4, 3 – pH 5

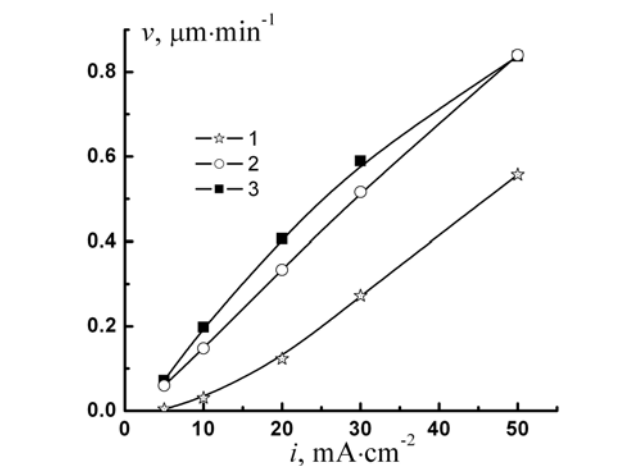


Fig. 4. Influence of current density on deposition rate at various pH for Solution 4, 1 – pH 3, 2 – pH 4, 3 – pH 5

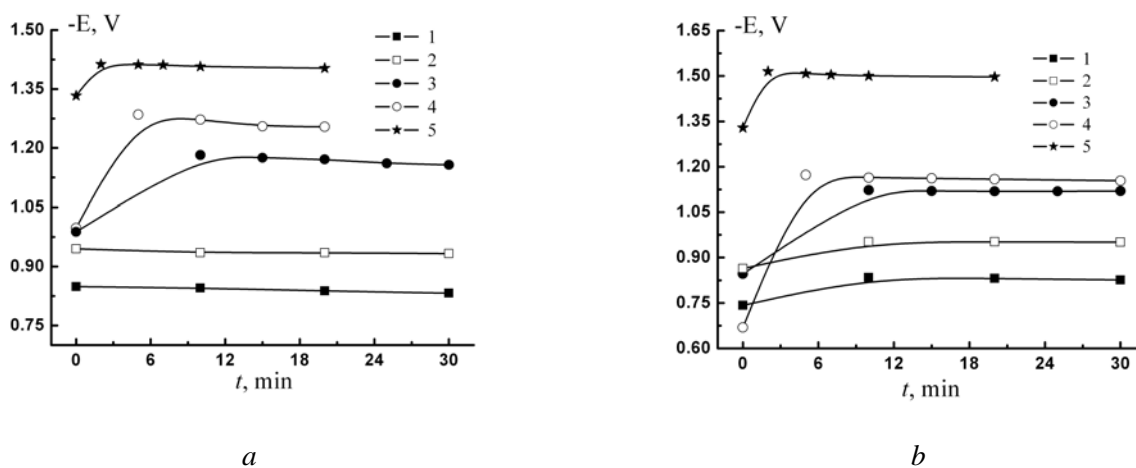


Fig. 5. The changes of electrodeposition potential during electrodeposition from Solution 1 (a) and Solution 2 (b) at pH 4 and different current densities: 1 – 2.5  $\text{mA}/\text{cm}^2$ , 2 – 5  $\text{mA}/\text{cm}^2$ , 3 – 10  $\text{mA}/\text{cm}^2$ , 4 – 15  $\text{mA}/\text{cm}^2$ , 5 – 25  $\text{mA}/\text{cm}^2$

**1.1.2 Morphology, Composition, and Structure of the Coatings.** Figure 6 shows the morphology of the obtained coatings and illustrates the influence of molybdenum content on the morphology. An increase in pH from 3 to 5 causes the increase in Mo content from 0.4 to 4.9 at.% (Solution 1). The same trend was obtained in Solution 2 where concentration of sodium molybdate is higher, that results a higher amount of Mo in the alloys. At relatively high (~5) pH and low amount of Mo in alloy, the deposits obtained at low current densities have needle- shaped surface (Fig. 6, Solution 1). The surface becomes more flat when current density increases even at the similar amount of Mo in alloys (pH 4, Solution 1). The increase of Na<sub>2</sub>MoO<sub>4</sub> concentration up to 0.012 M results in a flat surface even at low current densities and low amount of Mo in alloy (Fig. 6, Solution 2). Noticeably, the obtained “needle” - shaped structure of Co-Mo alloys also is typical for pure Co electrodeposited from citrate baths (see Fig. 7).

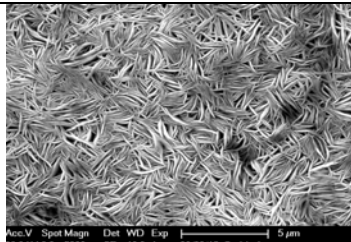
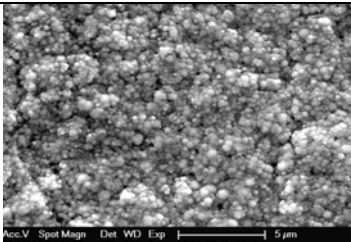
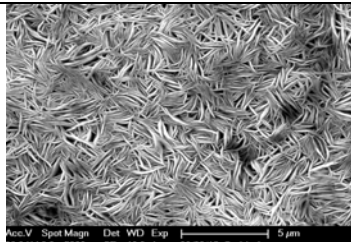
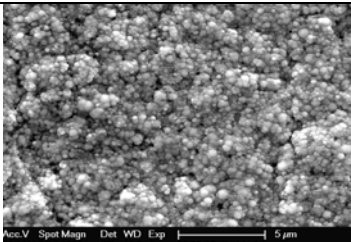
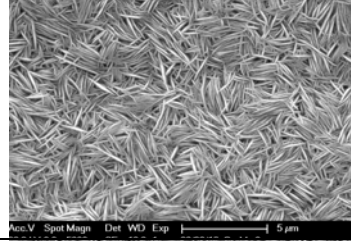
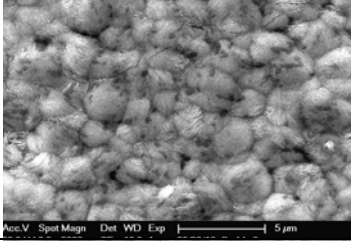
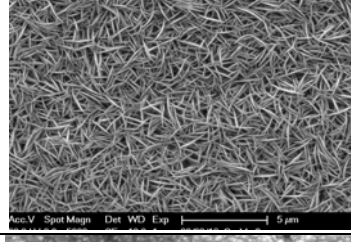
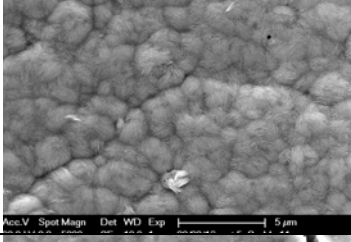
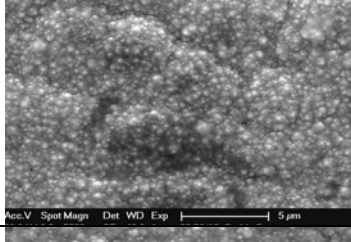
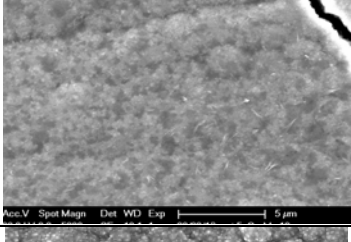
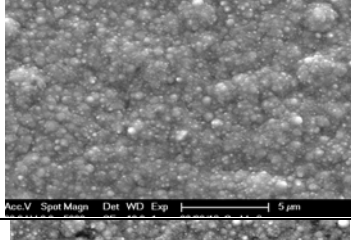
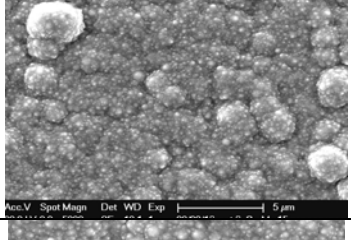
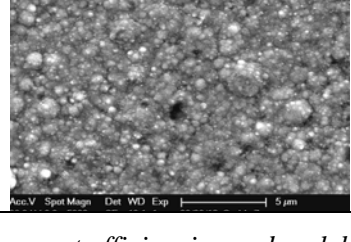
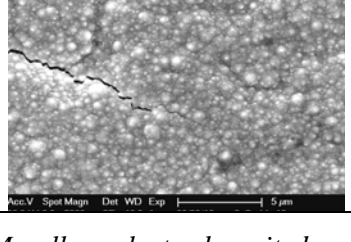
pH	<i>i</i> , mA/cm <sup>2</sup>	Solution 1		Solution 2	
			Mo content, at. %		
5	2,5		4.9	11.4	
5	5		3.6	8.1	
4	2,5		1.6	3.9	
4	5		1.8	5.3	
3	12.5		0.7	0.8	
3	25		0.4	1.0	

Fig. 6. SEM images, current efficiencies and molybdenum content of Co-Mo alloys electrodeposited on copper substrate from Solution 1 and 2, at different pH and current densities

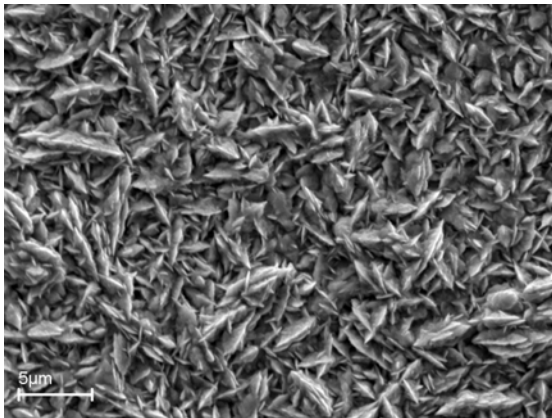


Fig. 7. SEM image of pure Co electrodeposited from the citrate baths

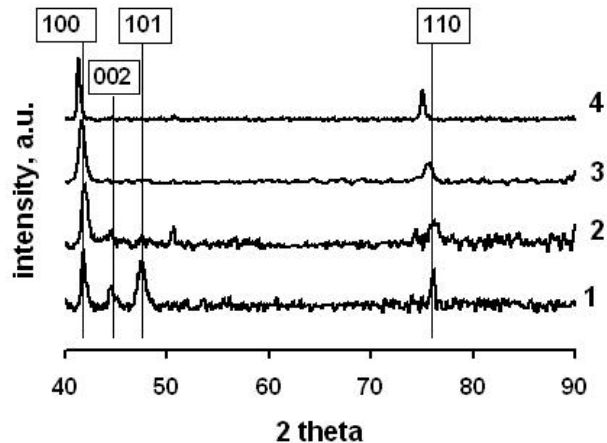


Fig. 8. XRD patterns for the electrodeposited from citrate baths pure Co (at  $5 \text{ mA cm}^{-2}$ ) and Co-Mo alloys. Lines mark positions of peaks attributed to the hexagonal Co in accordance with JCPDC data base. 1 – electrodeposited Co, 2 – Co-1.8 at.% Mo, 3 – Co-4.9 at.% Mo, 4 – Co-9.8 at.% Mo

The metallurgic Co has a structure of cubic lattice, whereas Co electrodeposited from citrate solutions has a hexagonal structure (see Fig. 8). As follows from the XRD patterns obtained for Co-Mo and presented in Fig. 8, positions of XRD peaks may be attributed to the structure of hexagonal Co of dominating planes {100} and {110} as well. At higher concentration of Mo in the alloy (9.8 at. %) the XRD peaks shift to lower angles that is caused by the increase of interplanar distance of formed lattice from  $2.16 \text{ \AA}$  (pure Co) to  $2.18 \text{ \AA}$  (Co-9.8 at.% Mo) for texture {100}, and from  $1.25 \text{ \AA}$  (pure Co) to  $1.26 \text{ \AA}$  (Co-9.8 at.% Mo) for texture {110}. Also, Co-Mo alloys may form an own structure, and in accordance with JCPDC data base such alloy with lowest content of Mo has a stoichiometry  $\text{Co}_3\text{Mo}$ . However, the positions of peaks for obtained Co-Mo alloys notwithstanding remain shifted by more than one degree from the positions characteristic for the stoichiometric  $\text{Co}_3\text{Mo}$  alloy. Thus, the solid solution of Co in  $\text{Co}_3\text{Mo}$  does not form at the contents of Mo in the alloys below 10 at. %, and mixture of Co and Mo in solid state is formed.

As it is shown in Fig. 8 and elsewhere [33], the broadening of peaks for the electrodeposited Co and electrodeposited Co-Mo alloys is similar; therefore the values of grain size for mentioned metals may be close to the values obtained for pure Co, i.e.  $\sim 40 \text{ nm}$ .

### 1.2. Co-Mo-P alloys study concerning template-assisted electrodeposition

The hydrogen overvoltage on Mo and Mo-containing alloys is lower than that for W and W-containing alloys, therefore the current efficiency and deposition rate for Mo-containing alloys is lower than that for corresponding W-containing alloys. Therefore, in some cases accelerators are used for the electrodeposition of Mo alloys, e.g. hydrazine [31, 34–35]. The accelerating rate of electrodeposition is important when template-assisted electrodeposition is concerned especially in the porous membranes or wafers with high aspect ratio. In this study we selected sodium hypophosphite as accelerator, because introduction of some amount of phosphorous into alloys does not have adversary effect on the surface morphology and corrosion properties of alloys even if the introduction of phosphorous occurs in cost of molybdenum [28, 31].

The effect of  $\text{NaH}_2\text{PO}_2$  on the polarization at various pH is shown in Fig. 9. It can be seen, the accelerating effect in the presence of  $\text{NaH}_2\text{PO}_2$  is more evident at lower values of pH although at pH 8 the acceleration takes place. It is caused probably by the easier reduction of hypophosphite ion at lower pH [36]:



and incorporation of P into alloy, that change kinetics of the Co and Mo codeposition. The similar effect was obtained in case of the electrodeposition ternary and quaternary tungsten alloys with Co, Ni and P [37].

The plateau is obtained on the polarization curves determined in acidic solutions at current density  $4\text{--}5 \text{ mA/cm}^2$ . The origin of plateau obtained on the polarization curves needs further investigations. Based on the simple estimations of limiting diffusion current taking into account that concentration of Co(II) is  $0.3\text{M}$ , the values of the diffusion limiting current have reach values  $45\text{--}50 \text{ mA/cm}^2$ . Preliminary study by

means of electrochemical impedance spectroscopy also does not show the slow diffusion stage because Warburg impedance does not appear in spectra. Most probably, the plateau is caused by the adsorbed intermediate compounds participating in the charge transfer reaction.

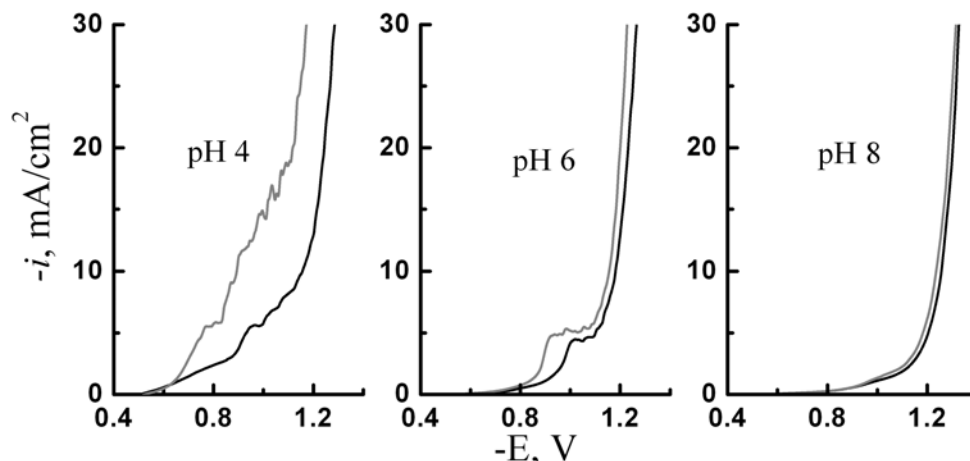


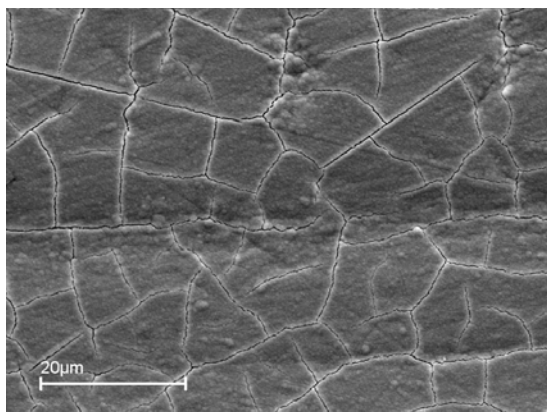
Fig. 9. Polarization curves registered on Co electrode from Solution 2 without  $\text{NaH}_2\text{PO}_2$  (black curves) and from Solution 3 with  $\text{NaH}_2\text{PO}_2$  (grey curves) at various pH. Potential scan rate  $5 \text{ mV s}^{-1}$

In all cases the currents are higher for electrodeposition in the present of  $\text{NaH}_2\text{PO}_2$  that is more favorable for electrodeposition in wafers that require long time, but quality of deposits obtained at pH 4 is worse than obtained at higher pH. The summation of the influence of the electrodeposition parameters and presence of hypophosphite on the quality of the obtained coatings at pH 6 is following:

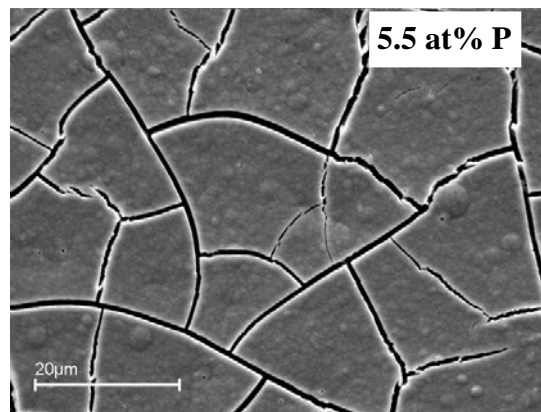
- the presence of phosphorous in the alloys obtained at direct current do not influence on the surface morphology (Fig. 9 a, b), but the deposition rate of ternary alloy is sufficiently higher than binary with molybdenum (table 1);
- ternary alloys containing P and electrodeposited in pulse current mode have less stress and cracks especially electrodeposited at low average current density (Fig. 9 c and d).

### 1.3. Electrodeposition into wafers

The thickness and content uniformity of electrodeposited metals and alloys applied in interconnect metallization of semiconductor wafers is of importance. Variations must be typically kept below  $\sim 3\%$ , with only a few mm edge exclusion. A number of process parameters, including the resistive copper seed and the wafer and anode configurations that are controlled by practical design considerations, adversely affect the current distribution [38]. An important issue during MEMS processing is the ability to plate and fill high aspect ratio structures evenly, and void free filled trench. Conformal plating is an even growth from all surfaces resulting in a deposit of equal thickness at all points.



a



b

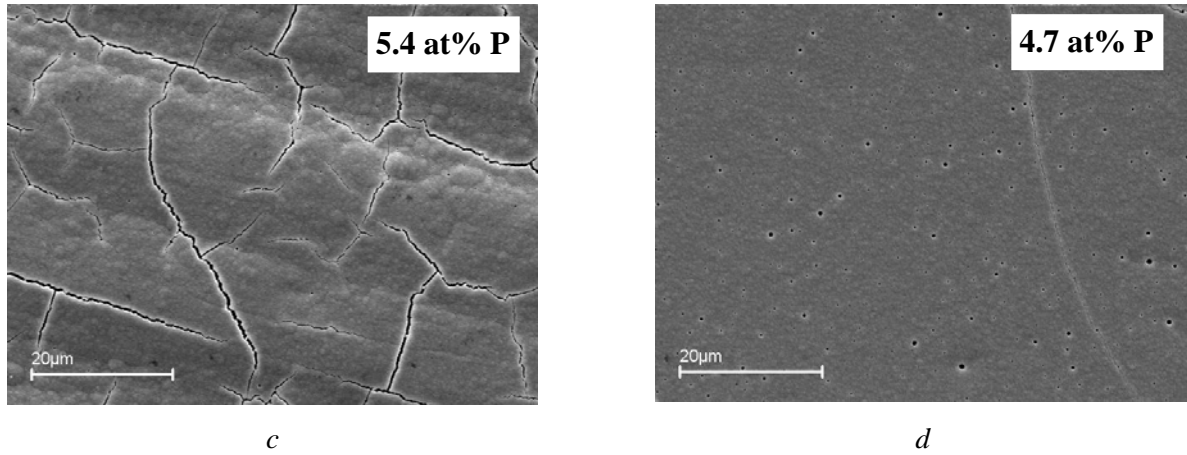


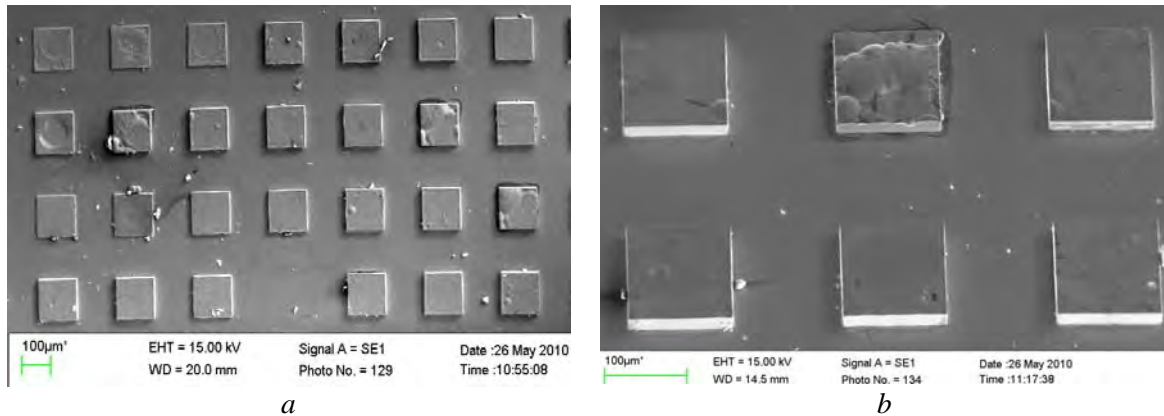
Fig. 10. SEM images of Co-Mo (a) and Co-Mo-P (b-d) alloys electrodeposited at pH 6 as mentioned in table

Table. The deposition parameters and composition of Co-Mo-P alloys obtained from Solution 3

Sample	pH	$C_{\text{NaH}_2\text{PO}_2}$ M	$i_{\text{avg}}$ , mA/cm <sup>2</sup>	$i_p$ , mA/cm <sup>2</sup>	$t_{\text{ON}}$ , s	$t_{\text{OFF}}$ , s	$v$ , µm/min	Composition at. %		
								Co	Mo	P
a	6	0	4	-	continuous	0	0.170	73.9	26.1	-
b		0.1	4	-	continuous	0	0.287	81.9	12.6	5.5
c			4	12	5	10	0.226	86.1	8.5	5.4
d			1.3	4	5	10	0.141	87.7	7.6	4.7

The wafers used in this study have photoresist layer over copper and patterned by the mask. This mask had opening squares whose size is 100 x 100 µm. Finally the Co-Mo-P alloys were plated under such optimal conditions: pH 6, averaged current density  $i_{\text{avg}} = 4$  mA/cm<sup>2</sup>, pulse current density,  $i_p = 12$  mA/cm<sup>2</sup> and  $t_{\text{ON}}/t_{\text{OFF}}$  is 5s/10s. These conditions correspond to the electrodeposition on bulk samples as shown in Fig. 9,c and table 1, sample c. As follows from the data presented in Table 1, As the amount of phosphorous in the alloys increases, the ratio of Mo:Co is reduced sufficiently, i.e. content of Mo in the alloy decreases sufficiently. The same effect was obtained also during electrodeposition W alloys with P, Co, and Ni, and was explained by surface blocking of adsorbed NaH<sub>2</sub>PO<sub>2</sub> intermediate that blocks available sites for the Mo or W intermediate [37].

The general and detailed SEM images of filling recesses after photoresist had been dissolved are shown in Fig. 11. As it is seen, the filling of the recesses is reasonable; the height of obtained posts is the same (Fig. 11,a and b); the surface is flat and consists on the fine crystallites (Fig. 11,e and f). The evenness of alloy composition distribution was estimated by measuring the composition in different places. It was found that for the resulting alloy with composition (in at. %) Co-9.3Mo-3.5P, the variation of analysis data does not exceeds ± 5% of determined value.



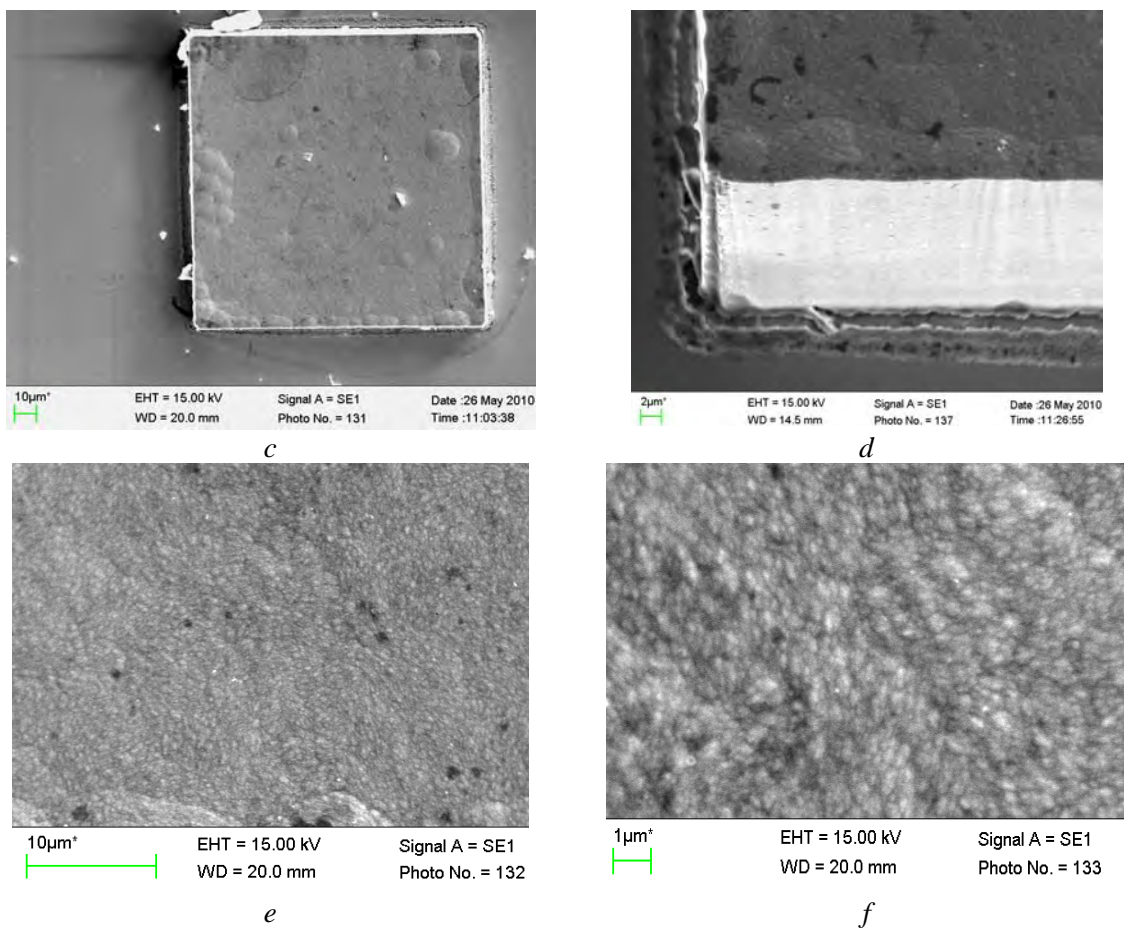


Fig. 11. SEM images of the big fragment of wafer (a), and detailed images of wafer with recesses filled by Co-Mo-P alloy (b, c and d), and the morphology of tops (e and f). Content of alloy Co-9.3 at.% Mo-3.5 at.% P

## Conclusions

1. The peculiarities of the Co-Mo and Co-Mo-P alloys electrodeposited from the citrate solutions at pH 4-6 was studied. Sodium hypophosphite was used as a source of phosphorous. The deposition rates for cobalt-molybdenum coatings are sufficiently lower than that for pure cobalt; this is chiefly due to lower hydrogen overvoltage on Mo-containing electrodes. The alloys containing up to 10 at.% of Mo were electrodeposited. The deposition rate increases sufficiently when ternary Co-Mo-P alloys are electrodeposited. The increase in deposition rate in the presence of NaH<sub>2</sub>PO<sub>2</sub> is more evident at lower values of pH. It is caused probably by the easier reduction of hypophosphite ion at lower pH and incorporation of P into alloy that change kinetics of the Co and Mo codeposition.

2. At relatively high (~5) pH and low amount of Mo in alloy, the coatings deposited at low current densities have needle-shaped surface. The surface becomes more flat when current density increases even at the similar amount of Mo in alloys (pH 4). The increase of Na<sub>2</sub>MoO<sub>4</sub> concentration up to 0.012 M results in a flat surface even at the low current densities and the low amount of Mo in alloy.

3. Positions of XRD peaks obtained for Co-Mo alloys are attributed to the structure of hexagonal Co of dominating planes {100} and {110}. At higher concentration of Mo in the alloy (9.8 at. %) the XRD peaks shift to lower angles that is caused by the increase of interplanar distance of formed lattice. The broadening of peaks for the electrodeposited Co and electrodeposited Co-Mo alloys is similar; therefore the values of grain size for mentioned metals may be close to the values obtained for pure Co, i.e. ~40 nm.

4. For the electrodeposition in wafers the low frequency current pulse mode was chosen. The alloy having composition (in at. %) Co-9.3Mo-3.5P was electrodeposited. The filling of the recesses is reasonable, and the height of obtained posts is the same, and the surface is flat and consists on the fine crystallites.

## Acknowledgements

The study is financed by the Lithuanian Research Council (contract MIP-134/2010) and Academy of Sciences of Moldova Nr. 09.819.05.02F. Also, authors are grateful to Prof. Mike Murphy (Louisiana State University) for wafers supply.



## REFERENCES

1. *Friend W.Z.* Corrosion of Nickel and Nickel Alloys // Wiley - Interscience, New York, 1980. vol. 248, p. 95–135.
2. *Chassaing E., Vu Quang K., Wiart R.* Mechanism of nickel-molybdenum alloy electrodeposition in citrate electrolytes // *Journal of Applied Electrochemistry*, 1989. vol. 19, No. 6, p. 839–844.
3. *Crousier J., Eyraud M., Crousier J.-P., Roman J.-M.* Influence of substrate on the electrodeposition of nickel-molybdenum alloys // *Journal of Applied Electrochemistry*, 1992. vol. 22, No. 8, p. 749–755.
4. *Podlaha E.J., Landolt D.* Induced Codeposition. II. // *Journal of the Electrochemical Society*, 1996. vol. 143, p. 885–892.
5. *Beltowska-Lehman E., Ozga P., Chassaing E.* Pulse electrodeposition of Ni-Cu-Mo alloys // *Surface and Coatings Technology*, 1996. vol. 78, p. 233–237.
6. *Cesiulis H., Budreika A.* Hydrogen evolution and corrosion of W and Mo alloys with Co and Ni // *Physicochemical Mechanics of Materials*, 2010. No. 8, 808–815.
7. *Fan C., Piron D.L., Sleb A., Paradis P.* Study of Electrodeposited Nickel-Molybdenum, Nickel-Tungsten, Cobalt-Molybdenum, and Cobalt-Tungsten as Hydrogen Electrodes in Alkaline Water Electrolysis // *Journal of the Electrochemical Society*, 1994. vol. 141, p. 382–387.
8. *Fan C., Piron D.L., Paradis P.* Hydrogen evolution on electrodeposited nickel-cobalt-molybdenum in alkaline water electrolysis // *Electrochimica Acta*, 1994. vol. 39, p. 2715–2722.
9. *Taylor W.P., Schneider M., Baltus H., Allen M.G.* A NiFeMo Electroplating Bath for Micromachined Structure // *Electrochemical and Solid-State Letters*, 1999. vol. 2, p. 624–626.
10. *Hu C.-C., Weng C.-Y.* Hydrogen evolving activity on nickel-molybdenum deposits using experimental strategies // *Journal of Applied Electrochemistry*, 2000. vol. 30, p. 499–506.
11. *Sato T., Takahashi H., Matsubara E., Muramatsu A.* Local Atomic Structure and Catalytic Activities in Electrodeposited Mo-Ni Alloys: Special issue on grain Boundaries, Interfaces, Defects and Localized Quantum Structures in Ceramics // *Materials Transactions*, 2002. vol. 43, p. 1525–1529.
12. *Zabinski P.R., Nemoto H., Meguro S., Asami K., Hashimoto K.* Electrodeposited Co-Mo-C Cathodes for Hydrogen Evolution in a Hot Concentrated NaOH Solution // *Journal of the Electrochemical Society*, 2003. vol. 150, C717–C722.
13. *Gómez E., Pellicer E., Vallés E.* Electrodeposited cobalt-molybdenum magnetic materials // *Journal of Electroanalytical Chemistry*, 2001. vol. 517, p. 109–116.
14. *Gómez E., Pellicer E., Vallés E.* Influence of the bath composition and the pH on the induced cobalt / molybdenum electrodeposition // *Journal of Electroanalytical Chemistry*, 2003. vol. 556, p. 137–145.
15. *Gomez E., Pellicer E., Valles E.* Microstructures of Soft-Magnetic Cobalt-Molybdenum Alloy Obtained by Electrodeposition Seed Layer/Silicon Substrates // *Electrochemistry Communications*, 2004. vol. 6, p. 853–859.
16. *Gomez E., Pellicer E., Duch M., Esteve J., Valles E.* Molybdenum Alloy Electrodeposits for Magnetic Actuation // *Electrochimica Acta*, 2006. vol. 51, p. 3214–3222.
17. *Myung N. V., Park D. Y., Schwartz M., Nobe K., Yang H., Yang C.-K., Judy J. W.* Electrodeposited Hard Magnetic Thin Films for MEMS Applications, Sixth International Symposium on Magnetic Materials, Processes and Devices // *Proceedings of the Electrochemical Society*, 2000. PV 2000–29.
18. *Gomez E., Kipervaser Z.G., Valles E.* A model for potentiostatic current transients during alloy deposition: cobalt/molybdenum alloy // *Journal of Electroanalytical Chemistry*, 2003. vol. 557, p. 9–18.
19. *Kuznetsov V.V., Bondarenko Z.V., Pshenichkina T.V., et al.* Electrodeposition of a cobalt-molybdenum alloy from an ammonia-citrate electrolyte // *Russian Journal of Electrochemistry*, 2007. vol. 43, No. 3, p. 349–354.
20. *Podlaha E.J., Landolt D.* Induced Codeposition: II. Mathematical Modeling of Ni-Mo Alloys // *Journal of the Electrochemical Society*, 1996. vol. 143, p. 893–899.
21. *Gomez E., Marin M., Sanz F., Valles E.* Nano- and micrometric approaches to cobalt electrodeposition on carbon substrates // *Journal of Electroanalytical Chemistry*, 1997. vol. 422, p. 139–147.
22. *Stepanova L.I., Purovskaja O.G., Azarko V.N., Sviridov V.V.* Peculiarities of Ni-Mo alloys electrodeposition from citrate electrolytes // *Proceedings of the Academy of Sciences of Belarus Series of chemical sciences*, 1997. No. 1, p. 38–43.
23. *Gomez E., Pellicer E., Valles E.* Developing plating baths for the production of cobalt-molybdenum films // *Surface & Coatings Technology*, 2007. vol. 197, p. 238–246.

24. *Subramania A., Sathiya Priya A.R., Muralidharan V.S.* Electrocatalytic cobalt–molybdenum alloy deposits // *International Journal of Hydrogen Energy*, 2007. vol. 32, No. 14, p. 2843–2847.
25. *Podlaha E.J., Landolt D.* Induced Codeposition: III. Molybdenum Alloys with Nickel, Cobalt and Iron // *Journal of the Electrochemical Society*, 1997. vol. 144, p. 1672–1680.
26. *Krohn A., Brown T.M.* Electrodeposition of Cobalt-Molybdenum Alloys // *Journal of the Electrochemical Society*, 1961. vol. 108, p. 60–64.
27. *Stasov A.A., Pasechnik S.A.* Nickel-molybdenum alloys electrodeposition from pyrophosphate electrolyte // *Izv. Vysh. Uch. Zav. Ser. Khim. Khim. Tekhnol.*, 1973. vol. 16, No. 4, p. 600–603 (in Russian).
28. *Donten M., Cesiulis H., Stojek Z.* Electrodeposition of amorphous/ nanocrystalline and polycrystalline Ni–Mo alloys from pyrophosphate baths // *Electrochimica Acta*, 2005. vol. 50, p. 1405–1412.
29. *Cesiulis H., Donten M., Donten M.L., Stojek Z.* Electrodeposition of Ni-W, Ni-Mo and Ni-Mo-W alloys from pyrophosphate baths // *Materials Science (Medziagotyra)*, 2001. vol. 7, no. 4, p. 237–241.
30. *Sidel'nikova S.P., Volodina G.F., Grabko D.Z., Dikusar A.I.* Electrochemical obtaining of Co-Mo coatings from citrate solutions containing EDTA: Composition, structure, and micromechanical properties // *Surface Engineering and Applied Electrochemistry*, 2007. vol. 43, No. 6, p. 425–430.
31. *Kublanovsky V., Bersirova O., Yapontseva Yu., Cesiulis H., Podlaha-Murphy E.* Cobalt–Molybdenum–Phosphorus Alloys: Electroplating and Corrosion Properties // *Protection of Metals and Physical Chemistry of Surfaces*, 2009. vol. 45, No. 5, p. 588–594.
32. *Sidel'nikova S.P., Dikusar A.I., Tsyntсарu N.I., Celis J.-P.* Effect of the electrodeposition conditions on the morphology, composition and physicomechanical properties of Co-Mo-P alloys // *Surface Engineering and Applied Electrochemistry*, 2008. vol. 44, No. 6, p. 428–435.
33. *Vasauskas V., Padgurskas J., Rukuiža R., Cesiulis H., Celis J.-P., Milčius D., Prosyčevs I.* Cracking Behavior of Electrodeposited Nanocrystalline Tungsten-Cobalt and Tungsten-Iron Coatings // *Mechanika (ISSN 1392 – 1207)*, 2008. vol. 72, No. 4, p. 21–27.
34. *Ernst D.W., Halt M.L.* Cathode Potentials during the Electrodeposition of Molybdenum Alloys from Aqueous Solutions // *Journal of the Electrochemical Society*, 1958. vol. 105, p. 686–692.
35. *Gromova V.A., Yapontseva Y.S., Bersirova O.L., Kublanovsky V.S.* The influence of electrolyte composition on the corrosion properties of Co-Mo electrolytic alloys // *Metallofiz. Noveishie Tekhnol.*, 2006. vol. 28, p. 5019–5026.
36. *Sotskaya N.V., Dolgikh O.V.* Kinetics of Cathodic Reduction of Hypophosphite Anions in Aqueous Solutions // *Russian Journal of Electrochemistry* 2005, vol. 41, No. 12, p. 1336–1340.
37. *Cesiulis H., Xie X.G., Podlaha-Murphy E.* Electrodeposition of Co-W Alloys with P and Ni. // *Materials Science-Medziagotyra*, 2009, vol. 15, issue. 2, p. 115–122.
38. *Malyshev E., Landau U., Chivilikhin S.* Modeling the deposit thickness distribution in copper electroplating of semiconductor wafer interconnects // *Presentation at the Metallization Symposium, AIChE Annual Meeting*, Nov. 17–18, 2003.

*Received 18.12.09*

### Summary

The aim of the present study is to investigate the electrodeposition of Co-Mo and Co-Mo-P alloys from the weakly acidic citrate bath and clarify factors influencing the deposition rate and composition of obtaining alloys, as well as their structure. Sodium hypophosphite was used as a source of phosphorous. The deposition rates for cobalt–molybdenum coatings are sufficiently lower than that for pure cobalt. The alloys containing up to 10 at.% of Mo were electrodeposited. The deposition rate increases sufficiently when ternary Co-Mo-P alloys are electrodeposited. The increase in deposition rate in the presence of NaH<sub>2</sub>PO<sub>2</sub> is more evident at lower values of pH. It is caused probably by the easier reduction of hypophosphite ion at lower pH and incorporation of P into alloy that change kinetics of the Co and Mo codeposition. Based on XRD data it is concluded that Co-Mo alloys has a structure of hexagonal Co of dominating planes {100} and {110}. At higher concentration of Mo in the alloy (9.8 at. %) the XRD peaks shift to lower angles that is caused by the increase of interplanar distance of formed lattice. The broadening of peaks for the electrodeposited Co and electrodeposited Co-Mo alloys is similar; therefore the values of grain size for mentioned metals may be close to the values obtained for pure Co, i.e. ~40 nm. For the electrodeposition in wafers the low frequency current pulse mode was chosen. The alloy having composition (in at. %) Co-9.3Mo-3.5P was electrodeposited. The filling of the recesses is reasonable, and the height of obtained posts is the same, and the surface is flat and consists on the fine crystallites.